Supplementary Information to *A model intercomparison of radiocarbon-based marine reservoir ages during the last 55 kyr including abrupt changes in the Atlantic Meridional Overturning Circulation*

Peter Köhler[1], Laurie Menviel[2], Frerk Pöppelmeier[3], Timothy J. Heaton[4], Edouard Bard[5], and Luke C. Skinner[6]

[1]Alfred-Wegener-Institut Helmholtz-Zentrum für Polar-und Meeresforschung, P.O. Box 12 01 61, 27515 Bremerhaven, Germany
[2]Climate Change Research Centre, Australian Centre for Excellence in Antarctic Science, University of New South Wales, Sydney, NSW, Australia
[3]Climate and Environmental Physics, Physics Institute and Oeschger Centre for Climate Change Research, University of Bern, Bern, Switzerland
[4]Department of Statistics, School of Mathematics, University of Leeds, Leeds, UK
[5]CEREGE, Aix-Marseille University, CNRS, IRD, INRAE, Collège de France, Technopole de l'Arbois BP 80, Aix en Provence Cedex 4, France
[6]Godwin Laboratory for Palaeoclimate Research, Earth Sciences Department, University of Cambridge, Downing Street, CB2 3EQ Cambridge, UK

Correspondence: Peter Köhler (peter.koehler@awi.de)

References

Heaton, T. J., Köhler, P., Butzin, M., Bard, E., Reimer, R. W., Austin, W. E. N., Ramsey, C. B., Grootes, P. M., Hughen, K. A., Kromer, B., Reimer, P. J., Adkins, J., Burke, A., Cook, M. S., Olsen, J., and Skinner, L. C.: Marine20 — the marine radiocarbon age calibration curve (0–55,000 cal BP), Radiocarbon, 62, 779–820, https://doi.org/10.1017/RDC.2020.68, 2020.

Köhler, P., Skinner, L. C., and Adolphi, F.: Radiocarbon cycle revisited by considering the bipolar seesaw and benthic ^{14}C data, Earth and Planetary Science Letters, 640, 118 801, https://doi.org/10.1016/j.epsl.2024.118801, 2024.

Reimer, P. J. and Reimer, R. W.: A Marine Reservoir Correction Database and On-Line Interface, Radiocarbon, 43, 461–463, https://doi.org/10.1017/S0033822200038339, 2001.

Skinner, L. C., Muschitiello, F., and Scrivner, A. E.: Marine Reservoir Age Variability Over the Last Deglaciation: Implications for Marine Carbon Cycling and Prospects for Regional Radiocarbon Calibrations, Paleoceanography and Paleoclimatology, 34, 1807–1815, https://doi.org/10.1029/2019PA003667, 2019.

Skinner, L. C., Primeau, F., Letsch-Thömmes, A., Joos, F., Köhler, P., and Bard, E.: Rejuvenating the ocean: mean ocean radiocarbon, CO_2 release, and radiocarbon budget closure across the last deglaciation, Climate of the Past, 19, 2177–2202, https://doi.org/10.5194/cp-19-2177-2023, 2023.

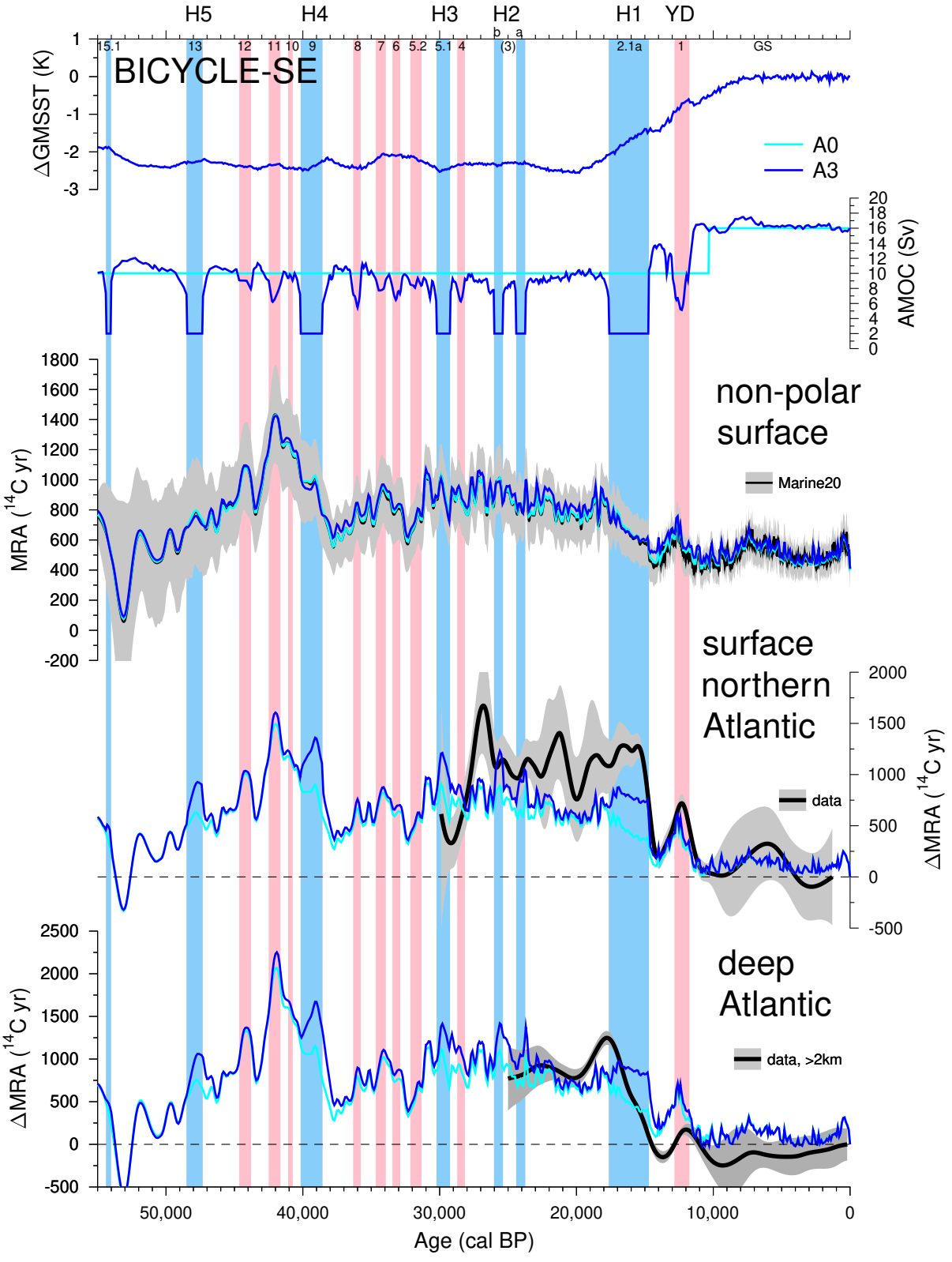

Figure S1. Results from the BICYCLE-SE carbon cycle box model. Prescribed changes in global mean sea surface temperature (GMSST) and AMOC strength leading to the simulated MRAs. Non-polar surface ocean are the 100 m deep so-called equatorial boxes in BICYCLE-SE, ranging from 40°S to 50°N or 40°N in Atlantic and Pacific, respectively. The surface North Atlantic is a 1 km deep box which covers all north of 50°N including the Arctic Ocean. The deep Atlantic box contains water below 1 km water depth reaching from 40°S to the North, including the Arctic Ocean. Data source: Marine20: Heaton et al. (2020); surface North Atlantic MRA: Skinner et al. (2019); deep Atlantic: Skinner et al. (2023) as compiled in Köhler et al. (2024). Vertical bands mark Heinrich events (blue) or non-Heinrich stadials (pink), see caption to Fig. 1 for details.

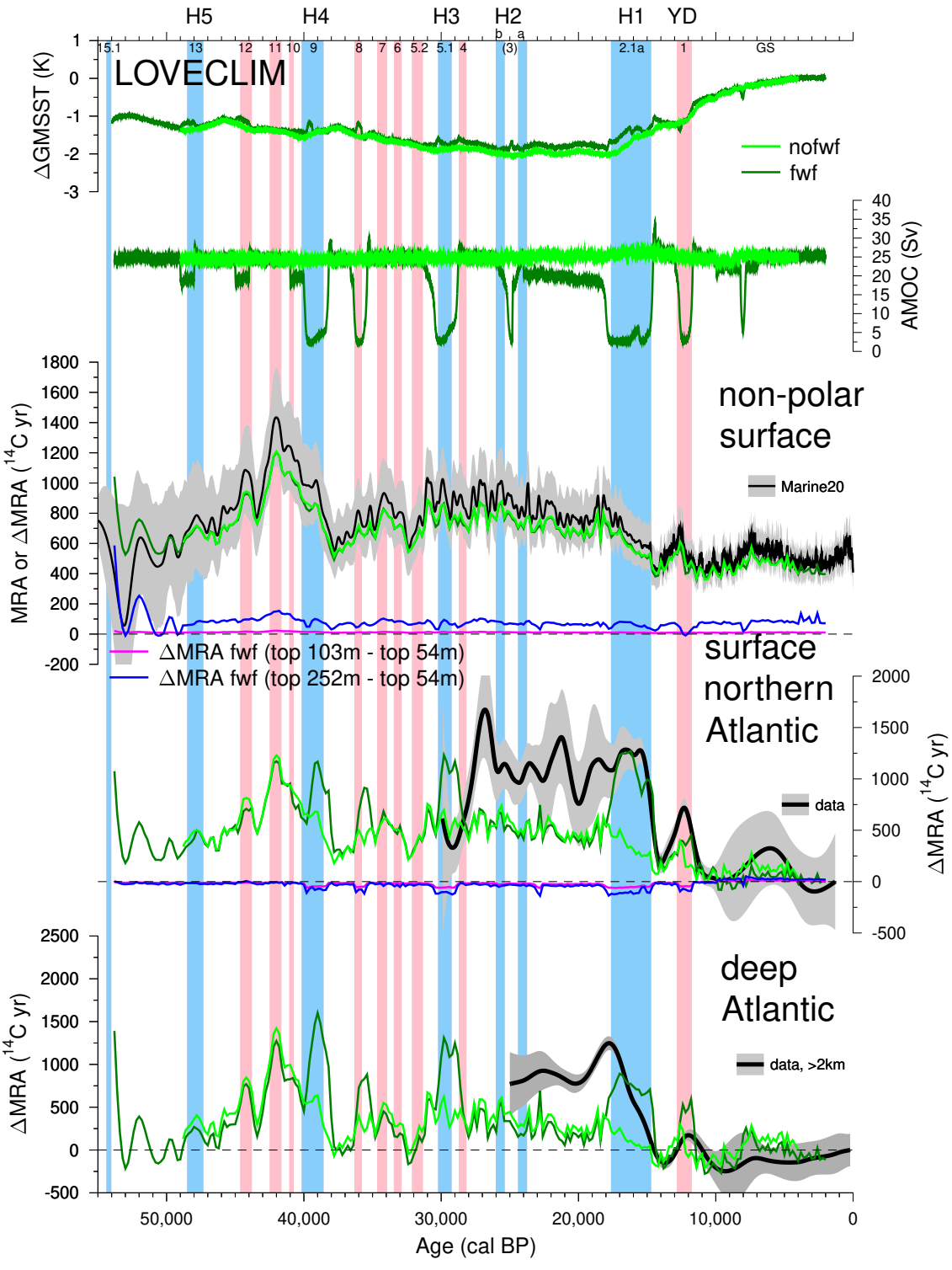

Figure S2. Results from the LOVECLIM EMIC. Changes in global mean sea surface temperature (GMSST) and AMOC strength leading to the simulated MRAs, both as 50-yr running mean. MRA of the non-polar surface ocean is based on the top 54 m ranging from 50°S to 50°N. The surface North Atlantic (top 54 m) covers all north of 50°N including the Arctic Ocean. Differences in MRA calculation when based on top 104 m or top 252 m water depth are shown for the non-polar surface and surface North Atlantic. The deep Atlantic contains water below 2 km water depth reaching 70°W–19°E, 40°S– 65°N. Data source: Marine20: Heaton et al. (2020); surface North Atlantic MRA: Skinner et al. (2019); deep Atlantic: Skinner et al. (2023) as compiled in Köhler et al. (2024). Vertical bands mark Heinrich events (blue) or non-Heinrich stadials (pink), see caption to Fig. 1 for details.

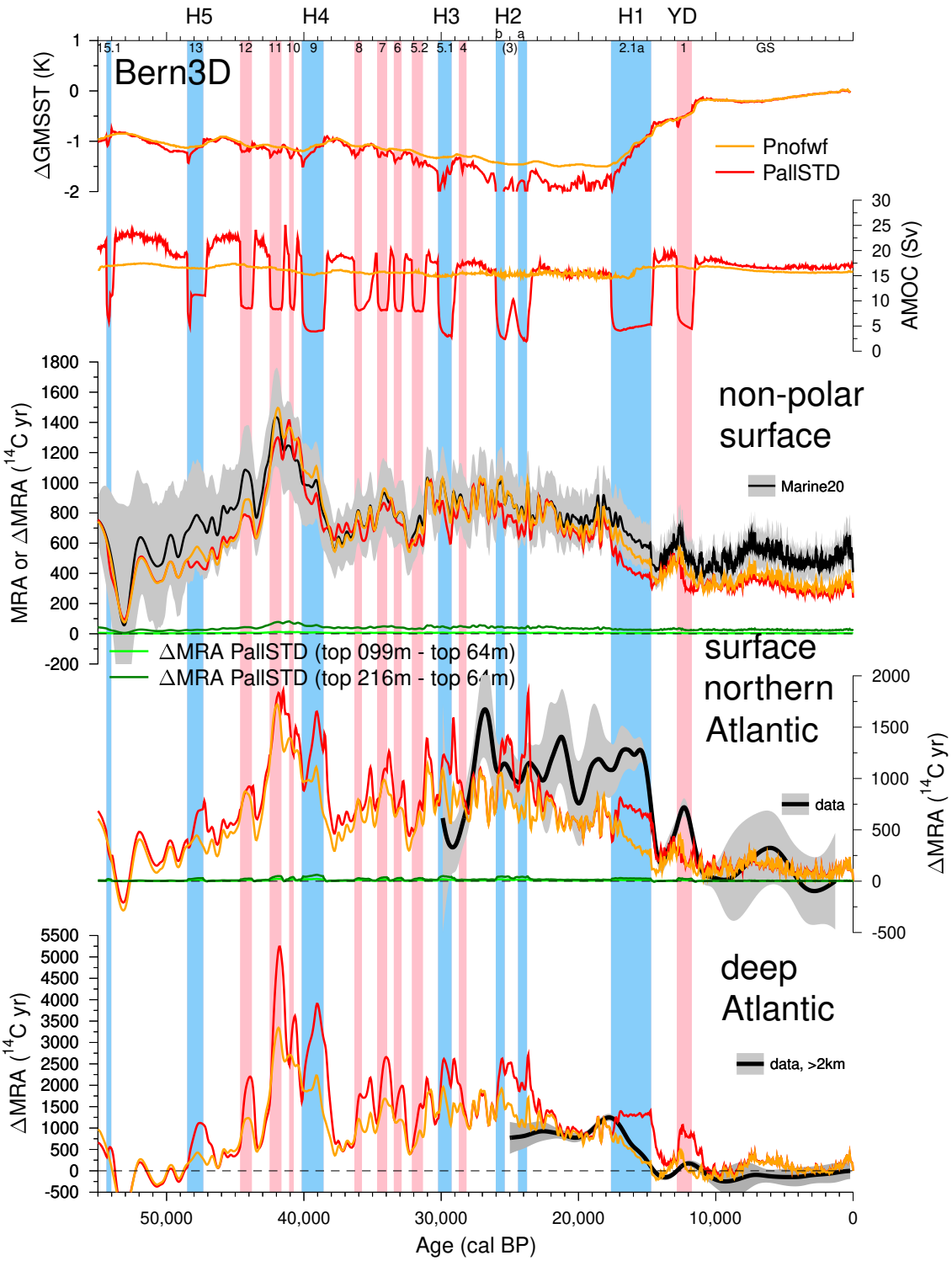

Figure S3. Results from the Bern3D EMIC. Changes in global mean sea surface temperature (GMSST) and AMOC strength leading to the simulated MRAs. MRA of the non-polar surface ocean is based on the top 64 m ranging from 50°S to 50°N. The surface North Atlantic (top 64 m) covers all north of 50°N including the Arctic Ocean. Differences in MRA calculation when based on top 99 m or top 216 m water depth are shown for the non-polar surface and surface North Atlantic. The deep Atlantic contains water below 2 km water depth reaching 35°S–70°N. Data source: Marine20: Heaton et al. (2020); surface North Atlantic MRA: Skinner et al. (2019); deep Atlantic: Skinner et al. (2023) as compiled in Köhler et al. (2024). Vertical bands mark Heinrich events (blue) or non-Heinrich stadials (pink), see caption to Fig. 1 for details.

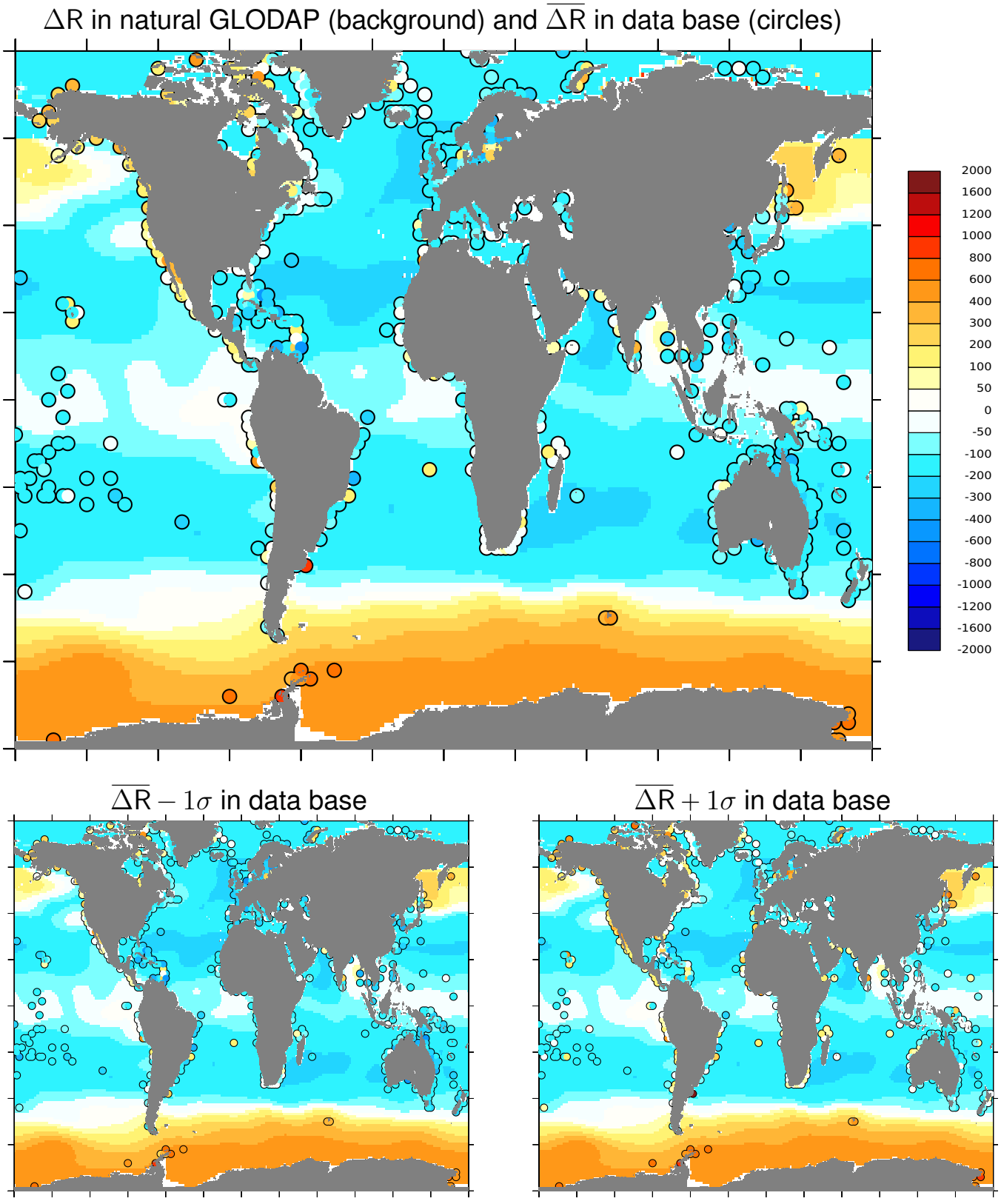

Figure S4. Marine surface ΔR (in ^{14}C yr), the local difference in MRA from the global value contained in Marine20. Background colors are from natural ^{14}C in GLODAP based on the top 50 m of the water column minus Marine20-based MRA at 0 kyr BP (407 ^{14}C yr). Circles are reconstructed ΔR from the data base http://calib.org/marine/ (Reimer and Reimer, 2001). Data have been averged for 2° in both latitude and longitude reducing 2000 entries into 609 plotted points. Subfigures differ only in the plotted ΔR from the data base (circles) as given in their headlines, showing either mean values ($\overline{\Delta R}$) or $\overline{\Delta R} \pm 1\sigma$. See methods for details.

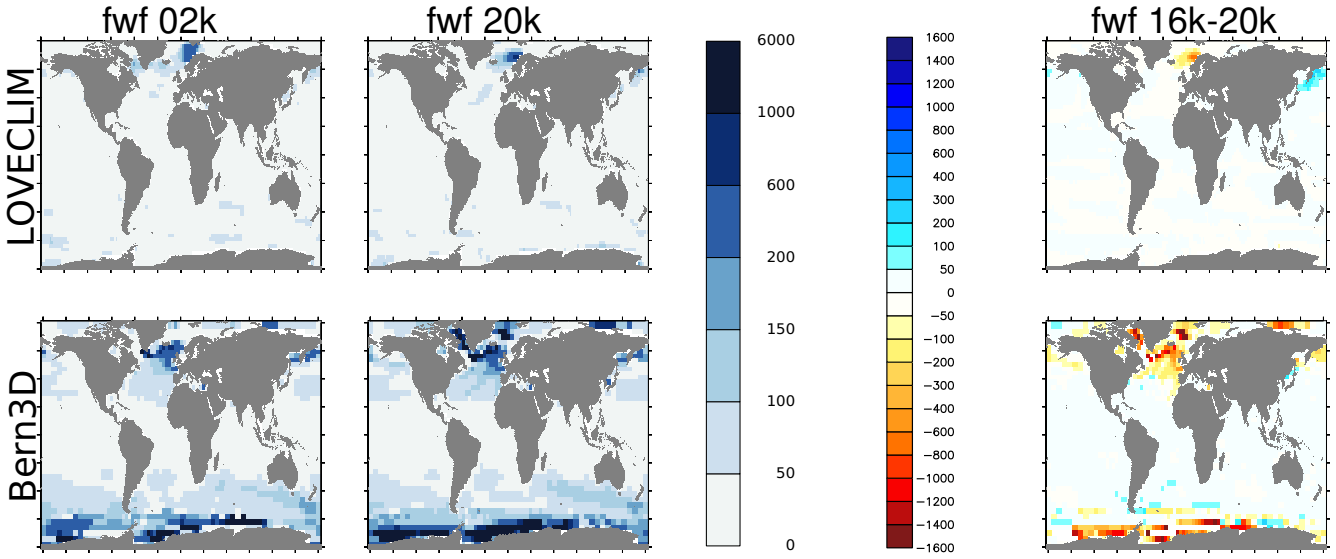

Figure S5. Annual mean mixed layer depth (MLD in m) for the simulation with freshwater fluxes (fwf) leading to reduced AMOC during stadials (scenarios: fwf@LOVECLIM; PallSTD@Bern3D). 1st column: 2 kyr BP; 2nd column: 20 kyr BP; 3rd column: difference in MLD (m) between 16 kyr BP and 20 kyr BP (16 – 20 kyr BP, or HS1–LGM). Criteria for MLD differ: LOVECLIM: depth of density difference from surface of $>$0.02 kg/m^3. Bern3D: mean of MLD in months January, February, March, July, August, September (depth of density difference from surface of $>$ 0.1 kg/m^3). Use left color-code (bluish) for absolute values and right color-code (red-to-blue) for differences.

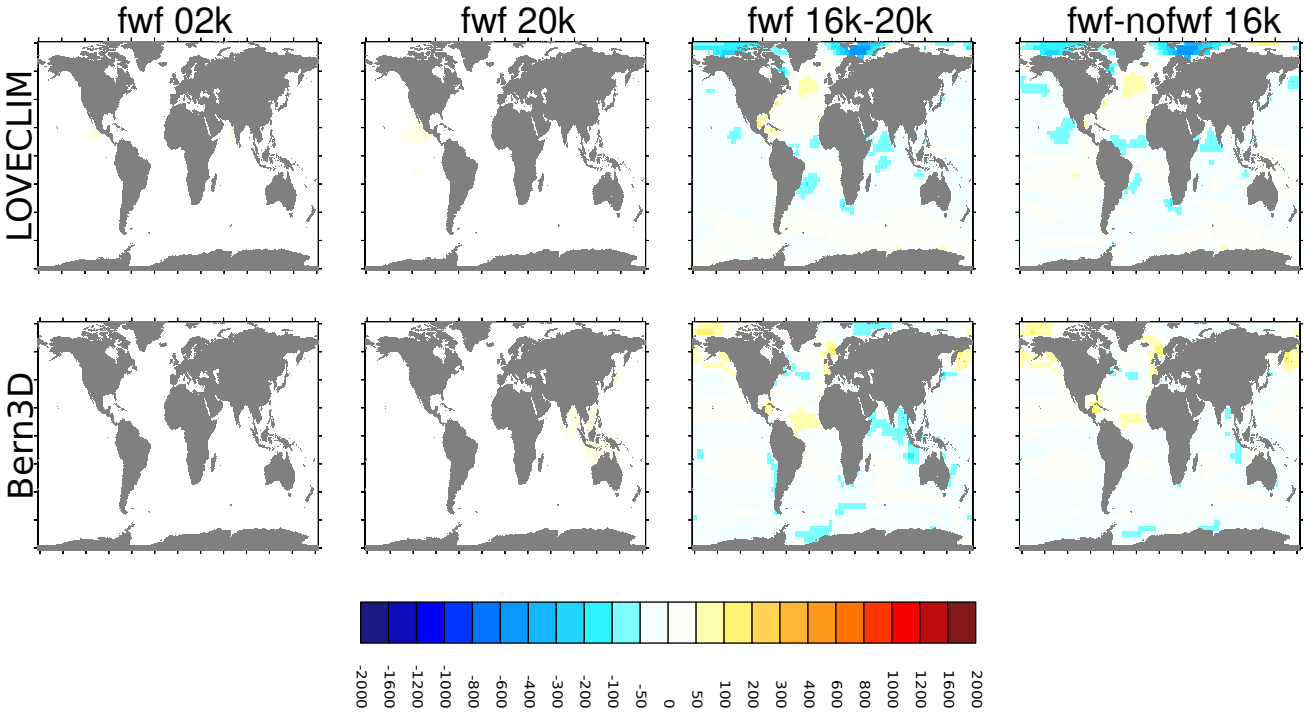

Figure S6. Differences in surface MRA (^{14}C yr) when calculations are based on roughly the top 200 m or roughly the top 50 m. 1st/2nd column: absolute value for 2 kyr BP and 20 kyr BP, respectively, for the simulation with freshwater fluxes (fwf) leading to reduced AMOC during stadials (scenarios: fwf@LOVECLIM; PallSTD@Bern3D). 3rd column: difference between 16 kyr BP and 20 kyr BP (16 – 20 kyr BP, or HS1–LGM). 4th column: difference at 16 kyr BP (HS1) between fwf and nonfwf (scenarios: A0@BICYCLE-SE, nofwf@LOVECLIM; Pnofwf@Bern3D).

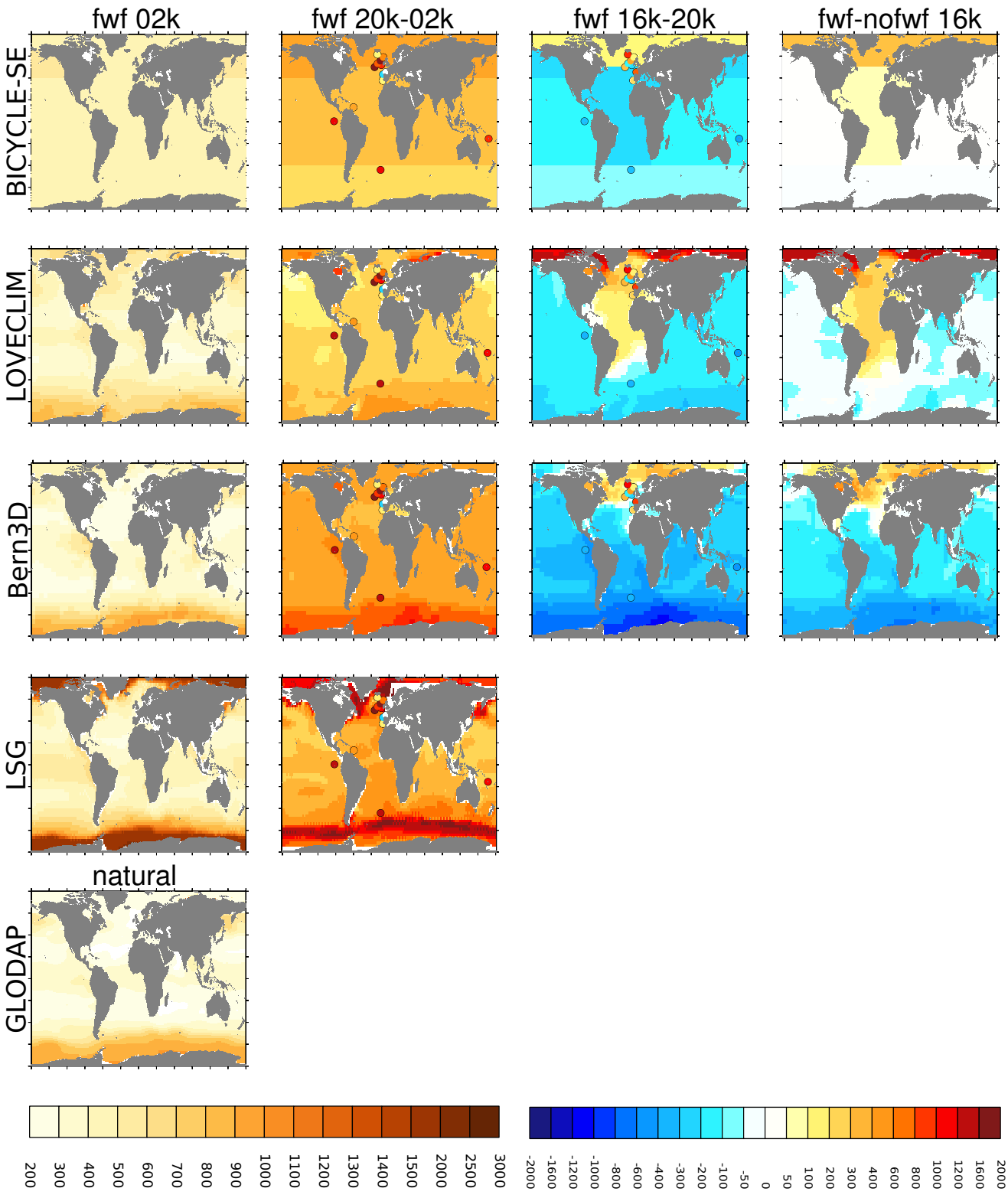

Figure S7. Combined overview on main results. Surface MRA (^{14}C yr) from all models (BICYCLE-SE: surface box; all else: roughly top 50 m) for the simulation with freshwater fluxes (fwf) leading to reduced AMOC during stadials (scenarios: A3@BICYCLE-SE, fwf@LOVECLIM; PallSTD@Bern3D) and scenario med@LSG 1st column: absolute value for 2 kyr BP (PI) and surface MRA from natural GLODAP. 2nd column: difference between 20 kyr BP and 02 kyr BP (LGM–PI). 3rd column: difference between 16 kyr BP and 20 kyr BP (HS1–LGM). 4th column: difference at 16 kyr BP (HS1) between fwf and nonfwf (scenarios: A0@BICYCLE-SE, nofwf@LOVECLIM; Pnofwf@Bern3D). Missing figures due to missing data for several configuration. Data-based reconstructions (Skinner et al., 2023): 19 points in the 2nd column (LGM, 19–21.8 kyr BP) and 13 points in 3rd column (HS1 (15–17.5 kyr BP) – LGM (19–21.8 kyr BP)). Use left color-code (brownish) for absolute values (1st column) and right color-code (blue-to-red) for differences (2nd–4th column).

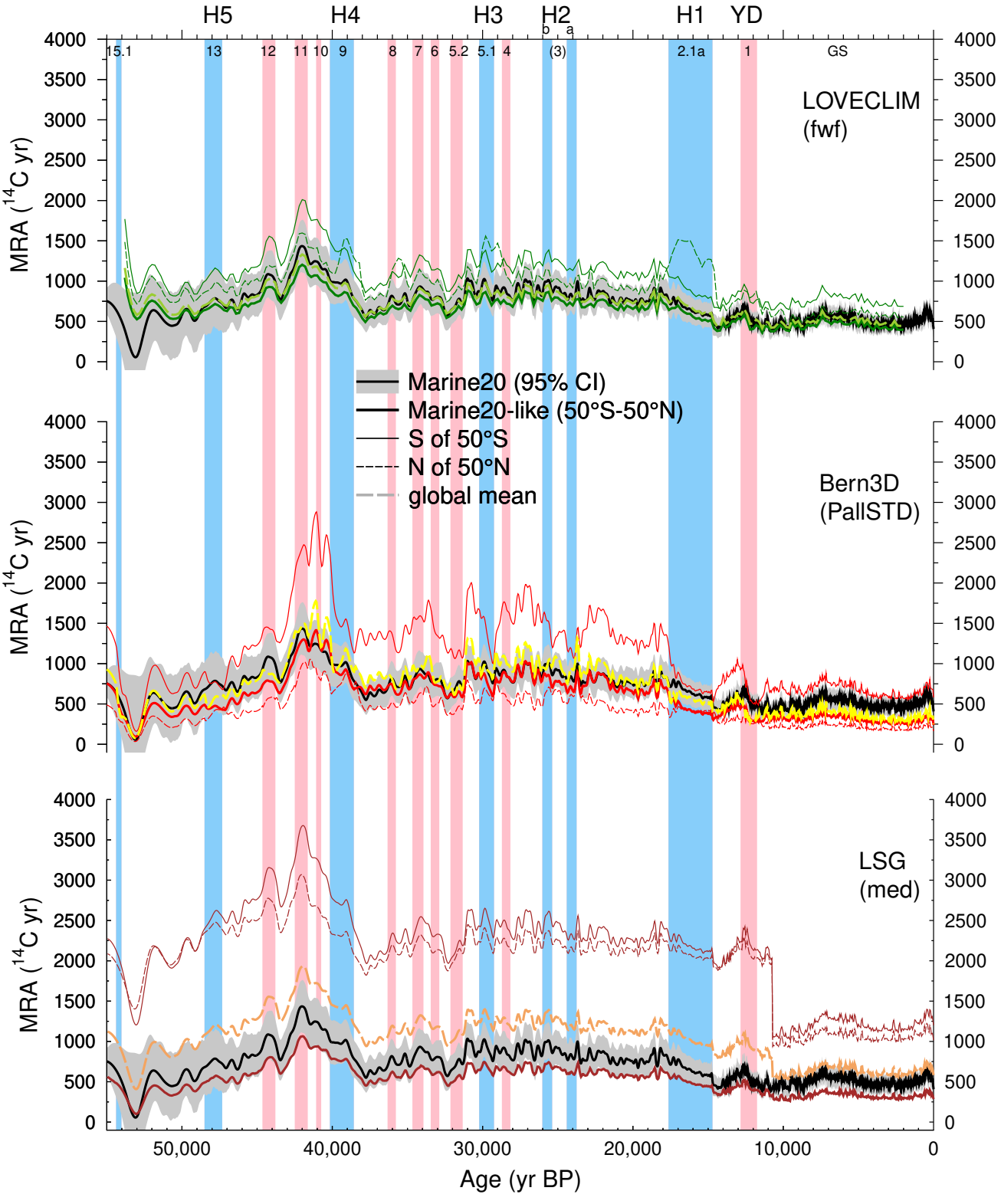

Figure S8. Towards global MRA. Comparing simulated MRA of the non-polar (Marine20-like; latitudes of $<50^{\circ}$), the high northern ($>50^{\circ}$N), the high southern ($>50^{\circ}$S) surface ocean and global mean MRA with Marine20 for different models. All model results are calculated from approximately the top 50 m of the ocean.

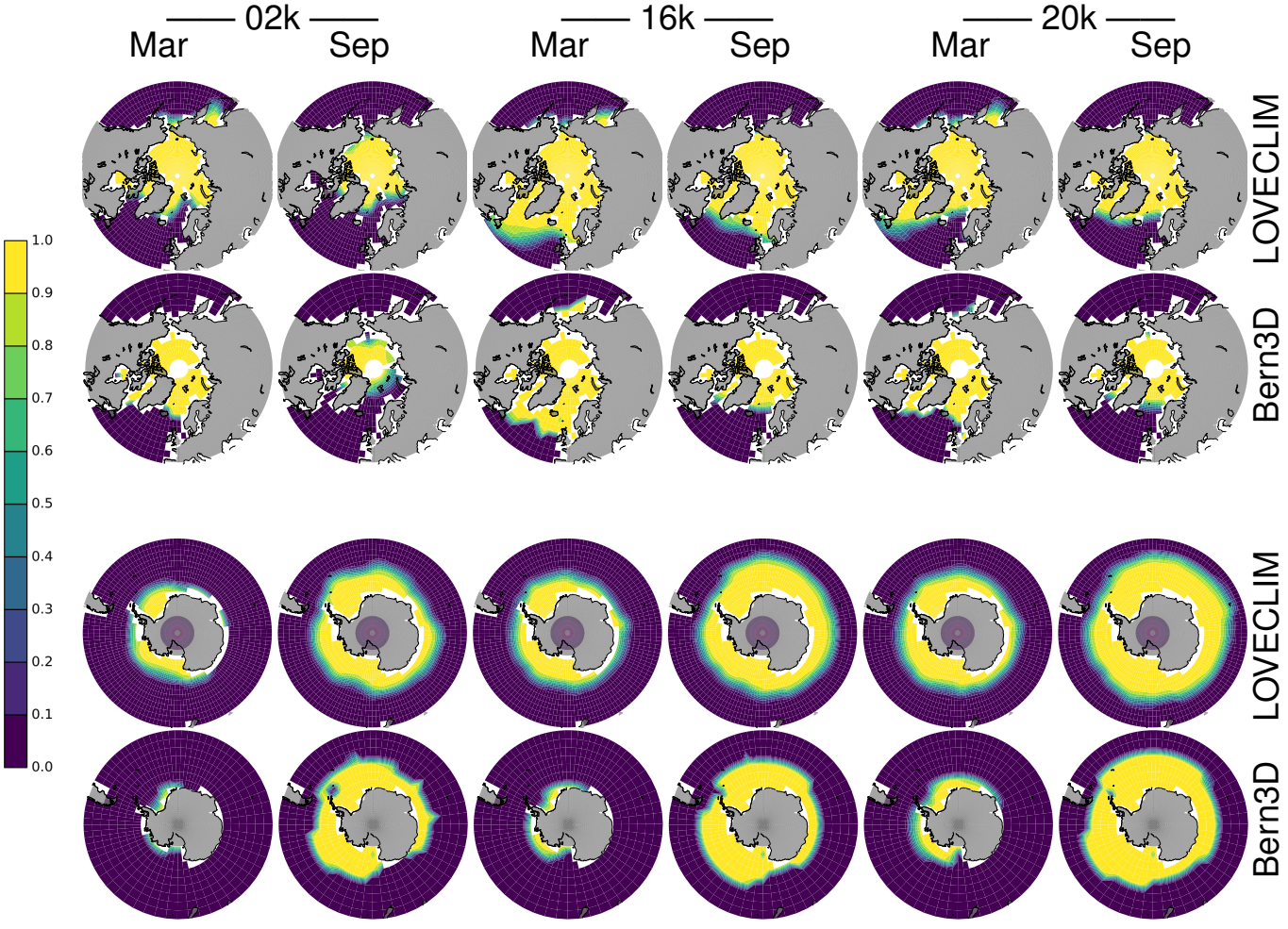

Figure S9. Sea ice fraction for March (Mar, 1st, 3rd, 5th column) and September (Sep, 2nd, 4th, 6th column) for three time windows (1st & 2nd column: 2 kyr BP; 3rd & 4th column: 16 kyr BP; 5th & 6th column: 20 kyr BP) and the two models LOVECLIM (1st & 3rd row) and Bern3D (2nd & 4th row) according to the labels. Northern (1st – 2nd row) and southern (3rd – 4th row) polar projections are showing areas $> 42.5^{\circ}$ latitudes. The white area at the North Pole misses simulation data (singularity) and the white zones within the sea ice area contain no ocean grid points.